Am J Cancer Res 2024;14(5):2088-2102
www.ajcr.us /ISSN:2156-6976/ajcr0155296

*Original Article*

# Loss of Lipocalin2 confers cisplatin vulnerability through modulating NF-κB mediated ferroptosis via ferroportin

Meibao Feng[1], Xuesong Wu[1*], Jing Zhang[1*], Pei Chen[1], Senmi Qian[2], Chengdong Chang[1]

*[1]Department of Pathology, The First Affiliated Hospital, School of Medicine, Zhejiang University, Hangzhou, Zhejiang, P. R. China; [2]Department of Gynecologic Oncology, Women's Hospital, School of Medicine, Zhejiang University, Hangzhou, Zhejiang, P. R. China. [*]Equal contributors.*

Received January 4, 2024; Accepted April 21, 2024; Epub May 15, 2024; Published May 30, 2024

**Abstract:** Cisplatin is a widely used anti-cancer drug. Unfortunately, many cancers often develop resistance, which contributes to tumor recurrence and poorly prognosis. Growing knowledge has suggested the therapeutic potential of ferroptosis in cancer. Lipocalin2 (LCN2) is demonstrated to be a critical iron metabolic factor and implies in ferroptosis. Here, we aim to explore its role in chemotherapy resistance. The influence of LCN2 on colorectal cancer (CRC) cell chemoresistance and ferroptosis were evaluated by in vitro and in vivo approaches. The interaction between LCN2, NF-κB and ferroportin (FPN) was assessed by western blots, immunohistochemistry and dual luciferase reporter assays. Results showed that LCN2 was highly expressed in tumor regression grade 1 (TRG1) cases than that in TRG3 specimens. Loss of LCN2 contributed to resistance to cisplatin-induced ferroptosis. Mechanistically, loss of LCN2 inhibited cisplatin sensitivity and cisplatin-induced ferroptosis through elevating FPN expression which was regulated by NF-κB, subsequently reducing $Fe^{2+}$ mediated Fenton reaction. Furthermore, FPN expression rate was much lower in TRG1 cases, and negative correlation between LCN2 and FPN expression was observed in clinical specimens. Collectively, low LCN2 expression enhances insensitivity of cisplatin to CRC cells via Fenton reaction mediated ferroptosis. LCN2/NF-κB/FPN pathway might be potentially utilized for chemoresistance strategy. LCN2 and FPN expression might be a promising biomarker of chemotherapy effect for CRC patients.

**Keywords:** Chemoresistance, biomarkers, Lipocalin2, ferroptosis, colorectal cancer

## Introduction

Although great advances in therapies have been received, colorectal cancer (CRC) is still the third most common malignancy worldwide and leading cause of cancer-related deaths globally, mostly due to its drug resistance and low response in patients [1].

Cisplatin is an extremely effective and widely used chemotherapy drug for the treatment of solid tumors. Unfortunately, many cancers often develop resistance in response to cisplatin treatment [2, 3]. Recent reports showed that ferroptosis was involved in the chemotherapy effect of cisplatin, the latter was indicated to provoke ferroptosis in various pathology processes [4].

Ferroptosis was a newly identified iron-dependent regulated cell death triggered by iron-catalyzed lipid peroxidation initiated by nonenzymatic (Fenton reactions) and enzymatic mechanisms [5]. Since being found, great knowledge has revealed the promising potential of ferroptosis as a novel therapeutic anticancer strategy, more importantly, its potential to overcome chemoresistance [6]. More interestingly, researches showed that ferroptosis can propagate among cells through a wave-like manner, suggesting its potent killing effect on neighboring cells [7-9]. Thus, identifying and exploring the clinical application of ferroptosis might be beneficial for enhancing our understanding of the ferroptosis mechanisms and tackling tumor progression.

Lipocalin2 (LCN2) is dysregulated in a variety of cancers and considered as a critical iron metabolic factor due to its iron-sequestering capacity [10]. Recently, LCN2 was identified as one of the antioxidant-related genes which is upregu-

https://doi.org/10.62347/MEYW3975

lated in various cellular stress conditions and involved in ferroptosis process. It was reported that LCN2 was a potential target in the cancer cachexia treatment by improving ferroptosis [11], and increased LCN2 activates inflammasome-ferroptosis processes in a mouse model of dry age-related macular degeneration [12]. Moreover, LCN2 was identified to be a core ferroptosis-related factor as it was highly correlated with ferroptosis-associated differentially expressed genes [13]. Furthermore, silencing of LCN2 was negatively related to ferroptosis events in ulcerative colitis which is closely associated with CRC [14]. Besides, LCN2 was observed to have an inhibitory effect on the system Xc-, and enhanced ferroptosis in intracerebral hemorrhage [15]. Remarkably, considering the ferrous iron ($Fe^{2+}$) and ROS dependency of ferroptosis, LCN2 might be involved in the regulation of ferroptosis.

Early work showed that the key factor of tumor progression, NF-κB, was elevated in LCN2 knockdown CRC cell lines [16], and was reported as a modulator of ferroptosis [17, 18]. However, its mechanisms in ferroptosis remains poorly understood.

Here, we provide evidence that loss of LCN2 expression acts as a negative regulator of ferroptosis by triggering NF-κB/FPN pathway underlying cisplatin treatment, more importantly, enhancing cisplatin vulnerability in CRC. Notably, LCN2 was negatively related with FPN expression and score of TRGs in patients undergoing chemotherapy. LCN2 and FPN expression might be potential biomarkers for predicting the chemotherapeutic effect of CRC patients.

## Material and methods

### *Cell culture and reagents*

The human CRC cell lines of HT-29, SW620, DLD1 and 293FT cells were generous gifts from Professor Maode Lai (Department of Pathology, School of Medicine, Zhejiang University); they were respectively cultured in RPMI 1640 and Dulbecco's Modified Eagle's Medium (DMEM) (Gibco, Grand Island, USA) supplemented with 10% fetal bovine serum (FBS, Excell Bioscience, Shanghai, China) and mycoplasma removal agent (1:100) and grown at 37°C under 5% $CO_2$. HT29 cells with LCN2 knockdown or knockout (designated as HT29-shLCN2 and HT29-LCN2-KO; vector control-SHB), and SW620 cells that stably expressed LCN2 (designated as OVER-LCN2; vector control-OB) were established by lentiviral shuttle vector. Cisplatin (cis, Cat No. HY-17394) was purchased from Med Chem Express (MCE, Hao yuan Bioscience, Shanghai, China), and cisplatin was incubated with corresponding cells for 30 μM (24/48 h). H2DCFDA (Cat No. HY-D0940) were from Med Chem Express (MCE, Haoyuan Bioscience, Shanghai, China). BODIPY 581/591 C11 (D3861) and Tetramethylrhodamine (TMRM, I34361) were obtained from Invitrogen (Thermo Fisher Scientific).

### *Reverse transcription-polymerase chain reaction (PCR) and real-time PCR analysis*

Total RNA was extracted from cells using TRIzol (Invitrogen, Carlsbad, CA) according to the manufacturer's protocol, and its concentration was measured using a spectrophotometer (Eppendorf, Hamburg, Germany). Total RNA (4 μg) was reverse-transcribed using the HiScript III All-in-one RT SuperMix Perfect for qPCR, and quantitative real-time PCR was performed using the ChamQ Universal SYBR qPCR Master Mix (Nanjing Vazyme Medical Technology Co., Ltd.) on a Bio-Rad CFX384 pcr quantitative analyzer (USA). The relative expression level was calculated using the $2^{-\Delta\Delta Ct}$ method and normalized by GAPDH expression. The sequences of the specific primers are listed in Table S1.

### *Western blot assay*

Cells were scraped, washed 3 times with PBS, and then lysed in RIPA buffer (Cat No. P0013B), which was purchased from beyotime Biotechnology, Shanghai, China.

Subsequently, the protein concentrations were determined by the Bradford method, and aliquots of the protein samples were stored at -80°C. Aliquots of protein extracts (15-50 μg) were separated on 10-12% SDS-polyacrylamide gels according to the protein molecular weights. Then, the proteins were elec-trophoretically transferred onto NC membranes (Merck Millipore, Darmstadt, Germany). After blocking with TBS-Tween 20 (TBST) containing 5% low-fat milk for 2 h in room temperature, the membranes were incubated with primary antibody overnight at 4°C. The membranes were

then incubated with secondary antibodies (Odyssey, Li-COR, Bioscience, Lincoln, USA) for 1 h at room temperature. Finally, the membranes were developed with the chemiluminescence image (Bio-Rad ChemiDoc MP system).

Antibodies against PTGS2 (AF7003, 1:1000), and hepcidin (HAMP, DF6492, 1:1000) were purchased from Affinity Biosciences (Shanghai, China), GAPDH (Cat No. 60004-1-Ig, 1:15000) and NF-κBp65 (Cat No. 80979-1-RR, 1:20000) were obtained from ProteinTech, Wuhan Sanying (Wuhan East Lake Hi-tech Development Zone, Wuhan, Hubei, P.R.C.). Ferroportin (FPN, 1:1000, NBP1-21502) antibody was purchased from Novus Biologicals (USA). Antibodies of LCN2 (ab41105, 1:1000) and NF-κBp65 (phospho S536, ab76302, 1:500) were from Abcam (Cambridge, England).

*Vector construction and small interfering RNA knockdown (siRNA)*

The lentiviral shuttle vector LV242-LCN2 was constructed to stably overexpress LCN2.

The lentiviral shuttle vector pLKO.1 was used to express shRNA. The target sequences of shRNA were: shLCN2-1: 5'-GAGTTCACGCTGGGCAACATTAAGA-3', shLCN2-2: 5'-GCTGGGCAACATTAAGAGTTA-3'.

For small interfering RNA (siRNA) knockdown of p65, cells were transfected with either p65 or negative siRNA (GenePharma, Shanghai, China) using the PowerFect siRNA in Vitro Transfection Reagent (Ver II, SignaGen Laboratories, Gaithersburg, MD) following the manufacturer's instruction. The siRNAs of p65 and FPN sequences are listed as: sip65-1: sense, 5'-GCACCAUCAACUAUGAUGATT-3', antisense, 5'-UCAUCAUAGUUGAUGGUGCTT-3'; sip65-2: sense, 5'-CCUCCUUUCAGGAGAUGAATT-3', antisense, 5'-UUCAUCUCCUGAAAGGAGGTT-3'. siFPN-1: sense, 5'-GUGGAAUCAUCCUGAUGAUTT-3', antisense, 5'-AUCAUCAGGAUGAUUCCACTT-3'; siFPN-2: sense, 5'-GGGAUUGGAUUGUUGUUGUTT-3', antisense, 5'-ACAACAACAAUCCAAUCCCTT-3'.

*Generation of LCN2-KO cell line*

The CRISPR/Cas9 technology was chosen to generate Lcn2-knockout (KO) HT29 cells. LCN2 CRISPR/Cas9 KO Plasmid (h) (sc-401838), LCN2 HDR Plasmid (h) (sc-401838-HDR) and the CRISPR/Cas9 scramble plasmid (ctr, sc-418922) were obtained from Santa Cruz Biotechnology. Each LCN2 CRISPR/Cas9 KO plasmid consists of a pool of 3 plasmids, each encoding the Cas9 nuclease and a target-specific 20 nt guide RNA designed for maximum knockout efficiency. Briefly, HT29 cells were co-transfected with CRISPR/Cas9 KO plasmids or the Ctr CRISPR/Cas9 plasmids and the HDR plasmids using Lipofectin 3000 (Thermo Fisher Scientific) according to the manufacturer's instruction. The single-clonal populations were then selected by flow cytometry and puromycin for 21 days. The absence of LCN2 in the clones generated was confirmed by Western blot analysis of protein extracts.

*Proliferation assay*

For the proliferation assays, $5 \times 10^3$ cells were seeded into 96-well plate with 100 μl RPMI 1640 supplemented with 10% FBS, using the Cell Counting Kit (CCK8, C0039, Beyotime Biotechnology, Shanghai, China) following the manufacturer's instructions and detected by a Luminometer (MD SpectraMax i3x, Austria) at 450 nm.

*Dual luciferase reporter assay*

Luciferase activity was measured as described previously [16]. In a brief, 490 ng of PGL4.21-FPN-luc or PGL4.21-luc and 10 ng of Renilla luciferase plasmids were co-transfected into corresponding cells. After 24 h of treatment, luciferase activity was assayed using the Dual Luciferase Assay System (Promega, Madison, WI) according to the manufacturer's protocol on a Luminometer (MD SpectraMax i3x, Austria). Each firefly luciferase value was corrected for its co-transfected Renilla luciferase value.

*Ferrous iron ($Fe^{2+}$) level detection and mitochondrial membrane potential (MMP) measurement*

To detect intracellular $Fe^{2+}$ and MMP levels, FerroOrange (Dojindo) and TMRM (Invitrogen) were used according to the manufacturer's protocol. Corresponding cells were seeded in 96-well plates and treated with cisplatin for the indicated time and stained with a final concentration of 1 μM FerroOrange and 0.1 μM TMRM respectively, for 30 minutes at 37°C protected

from light, then detected by a Luminometer (Bio-Tek Synergy Neo2, USA).

*ROS measurement*

The level of intracellular and total ROS was respectively evaluated by the uptake of H2D-CFDA and BODIPY 581/591 C11 (Invitrogen). To visualize the lipid ROS, cells were seeded in 96-well plates and treated with the designate conditions, then cells were stained with H2DCFDA or BODIPY followed the manufacturer's instructions. After 30 minutes in the dark, the cells were detected by a Luminometer (Bio-Tek Synergy Neo2, USA).

*In vivo mouse tumorigenicity assay*

Five-week-old male BALB/c mice were purchased from Hangzhou medical college, Hangzhou, China. The mice were housed in individually ventilated cages and supplied with sterilized food, water, and bedding. The mice were maintained at environmental temperature and humidity ranges from 21 to 26°C, and from 50% to 70%, respectively. HT29-SHB, shLCN2-1 and LCN2-KO cells ($5 \times 10^6$) in 200 μl PBS were inoculated subcutaneously into the right shoulders of BALB/c mice. Mice were randomly allocated into different groups and intraperitoneally injected with cisplatin (MCE, HY-17394) at a dose of 15 mg/kg or the same amount of saline water for control every other day, when the tumor volume reaches 100-150 $mm^3$. Tumor length and width were measured with calipers, and tumor volumes were calculated according to the equation: V ($mm^3$) = ½ [width$^2$ ($mm^2$) × length (mm)]. Growth curves were plotted based on mean tumor volume within each experimental group at the indicated time points. Tumor growth was observed for 15 days. Ethics approval and consent to participate all human tissues and data and animals involved in this study were approved by the Ethics Committee of the First Affiliated Hospital, School of Medicine, Zhejiang University.

*Immunohistochemical staining and scoring*

Immunohistochemical staining by Envision method was performed on formalin-fixed paraffin-embedded slides, which had been dewaxed and rehydrated before antigen retrieval step [16]. Each specimen was scored according to the proportion of positive tumor cells: 0, negative or < 5%; 1, 5-25%; 2, 26-50%; 3, 51-75%; 4, > 75%. The score of staining intensity was kept in range of 0 to 3 based on: 0 for no staining, 1 for weak staining, 2 for moderate staining and, 3 for strong staining.

The chemotherapy efficacy was evaluated using the tumor regression grade (TRG) scoring system by two independent pathologists, with score of 1 (only minimal residual tumor cells were left, with clear evidence of post-chemotherapy response) and 3 (large areas of residual tumor cells were observed, with no clear evidence of post-chemotherapy response).

Antibodies and dilutions are as below: LCN2 (dilution 1:200, ab41105, Abcam, cytoplasm, n = 17 (TRG1), n = 20 (TRG3)), and Ferroportin (FPN, dilution 1:400, NBP1-21502, Novus, cytomembrane and cytoplasm, n = 17 (TRG1), n = 20 (TRG3)). Subsequently, LCN2 and FPN staining were defined as negative (score 0) and positive (scores ≥ 1).

LCN2 was defined as low (score < 6) and high (score ≥ 6), while FPN was defined as low (score < 4) and high (score: ≥ 4). Immunohistochemical staining were from the database in pathology department of the first affiliated hospital, School of medicine, Zhejiang University. Clinical specimens of all 37 patients were enrolled with informed consent in accordance with a protocol approved by the Ethics Committee of the first affiliated hospital, School of medicine, Zhejiang University.

*Statistical analysis*

All statistical analyses were performed using Prism 8.0 (GraphPad Software) and SPSS (version 24.0; IBM, New York, NY). For results from cell lines, all data are reported as mean ± S.D. Differences between means were determined using the two-tailed, unpaired Student's t-tests. Correlation coefficients were calculated by the Spearman rank correlation test and were considered significant at $P < 0.05$.

## Results

*LCN2 is involved in regulating ferroptosis in CRC cell lines*

LCN2 participates in the development of various tumors and plays an important regulatory role in innate immune responses, for its ability

of inhibiting bacterial growth by competing with bacteria for binding to ferrous iron ($Fe^{2+}$), which is a critical factor in ferroptosis. To explore the involvement of LCN2 in ferroptosis, we first constructed an LCN2 knockdown cell line (HT29-SHB/shLCN2) and found that the expression of the critical ferroptosis marker PTGS2 was significantly downregulated (**Figure 1A**). The mRNA levels of ferroptosis regulatory factors, including GPX4, SLC7A11, and FTH1, exhibited a notable increase, whereas ACSL4 and TFRC demonstrated significant reduction (**Figure 1B**). Further examinations also indicated that shLCN2 decreased the levels of intracellular and total lipid ROS, as well as mitochondrial membrane potential (MMP) hyperpolarization (**Figure 1C-E**). To further confirm the origin of lipid ROS, we next measured iron content and FPN in the treated cells, which are the crucial regulators of iron metabolism. As expected, results revealed that the content of $Fe^{2+}$ was significantly decreased, and FPN expression and promoter activity were markedly increased (**Figure 1A**, **1F**, **1G**). Similar changes of FPN expression and activity of promoter were also observed in LCN2 knockout (LCN2-KO) cells (Figure S1A, S1B). The mRNA levels of the key regulatory factors of ferroptosis and the changes in lipid ROS, MMP, and $Fe^{2+}$ levels in LCN2-KO cells were consistent with the trend obtained in shLCN2 cells (Figure S1C-G). Furthermore, in the constructed LCN2 overexpression cells (SW620-OB/OVER-LCN2), it was also showed a significant increase of PTGS2 expression and corresponding ferroptosis markers, and a decrease in FPN expression (**Figure 2A**, **2B**). Likewise, lipid ROS levels and intracellular $Fe^{2+}$ contents were upregulated, MMP was hyperpolarized in OVER-LCN2 cells (**Figure 2C-F**). The above results suggest that LCN2 may be involved in ferroptosis by modulating FPN expression in CRC cells.

*Downregulation of LCN2 expression ameliorates the sensitivity of CRC to cisplatin treatment*

Cisplatin is a classic chemotherapy drug widely used in the clinical treatment of a series of cancers. To explore whether LCN2 was involved in the sensitivity of CRC to cisplatin. We first measured LCN2 expression in the presence of cisplatin. As expected, cisplatin can significantly upregulate the expression of LCN2 in CRC cells (**Figure 3A**). Next investigation revealed that cisplatin can significantly reduce the survival and proliferation ability of CRC cells. shLCN2 or LCN2-KO can slightly reverse the effect of cisplatin in cell viability (**Figure 3B**, **3C**). Further exploration showed that shLCN2 and LCN2-KO could significantly increase tumor volumes in mouse tumor xenografts, while that were markedly decrease under the treatment of cisplatin. Consistent with our speculation, shLCN2 and LCN2-KO could significantly restore tumor volumes and proliferation ability in cisplatin treatment, suggesting that loss of LCN2 impaired the anti-tumor effect of cisplatin in vivo (**Figure 3D**, **3E**). Thus, it is necessary to further explore the role of LCN2 played in the process of cisplatin treatment.

*Lack of LCN2 expression prevents cisplatin-stimulated ferroptosis*

We first investigate the role of cisplatin in ferroptosis of CRC. We measured changes of ferroptosis-related markers in the treatment of cisplatin. Consistent with previous reports, cisplatin could induce ferroptosis by increasing the levels of PTGS2 expression, lipid ROS and MMP hyperpolarization (**Figure 4A-D**). Similar changes were obtained in mRNA levels of ferroptosis-related genes (Figure S2).

Next, corresponding cells were detected to further confirm the role of LCN2 in cisplatin-induced ferroptosis. As results shown in **Figures 4A-D** and S3A-D, lack of LCN2 significantly prevented the cellular changes, such as elevated expression of PTGS2, increased level of lipid ROS and MMP, as well as mRNA changes of ferroptosis-related genes, caused by cisplatin treatment (Figure S2).

*FPN was involved in cisplatin-induced ferroptosis mediated by loss of LCN2*

Further investigation showed the reduced level of $Fe^{2+}$ and the increased FPN expression and its promoter activity in cells with loss of LCN2 expression. Unexpectedly, cisplatin treatment enhanced the inhibition effect of lack of LCN2 on $Fe^{2+}$ content (**Figures 4E-G**, S3E, S3F). Furthermore, the levels of lipid ROS, MMP and $Fe^{2+}$ in shLCN2 and LCN2-KO cells were markedly provoked and impaired the inhibition effect of shLCN2 on cisplatin-induced ferroptosis after decreasing FPN expression by specific siRNA (**Figure 5A-H**). Moreover, according to TCGA database, high LCN2 and low FPN expression

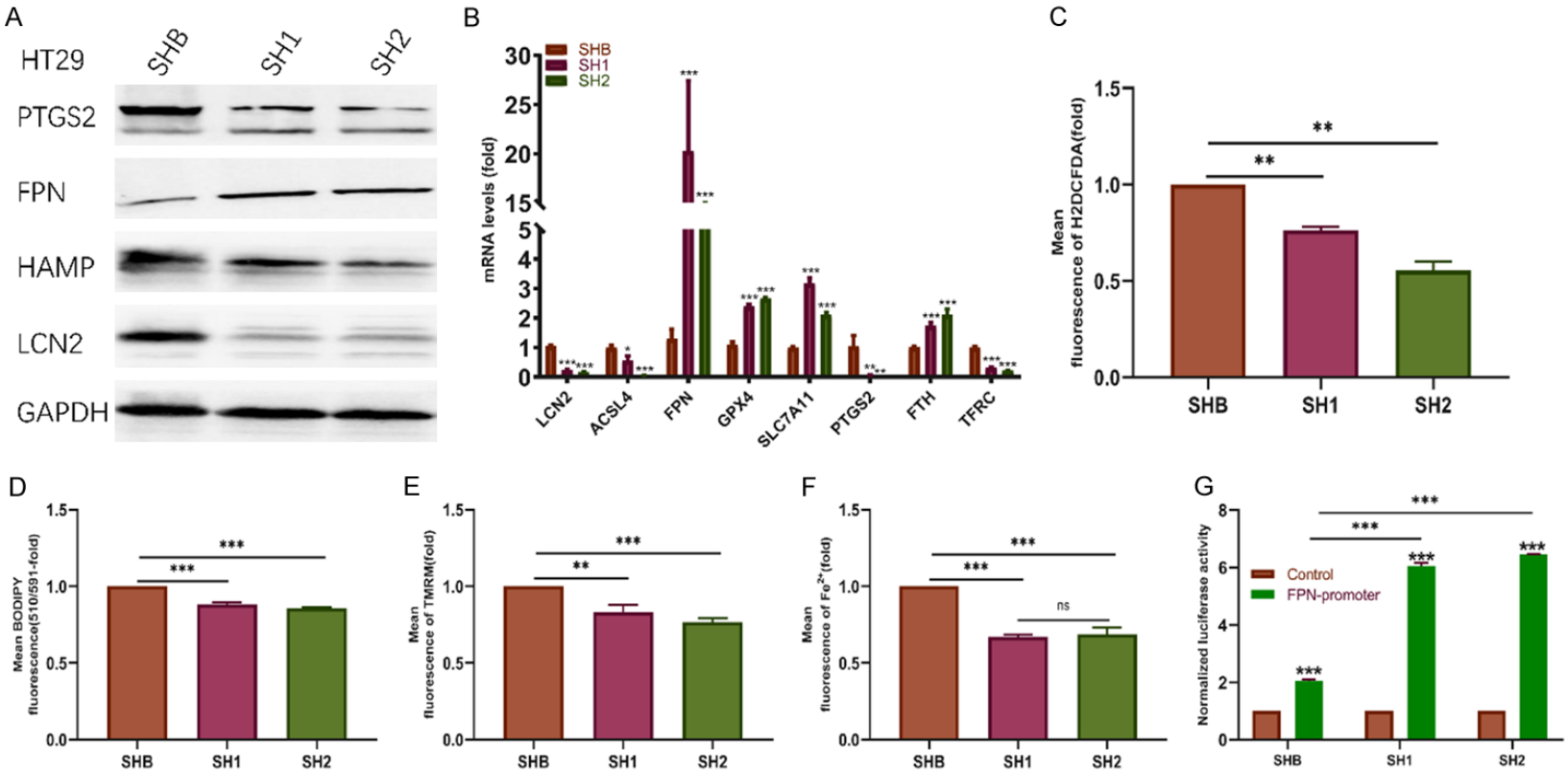


**Figure 1.** Knockdown of LCN2 expression suppresses ferroptosis characteristics in vitro. Western blots detection of Lipocalin2 (LCN2), PTGS2, ferroportin (FPN), and hepcidin (HAMP) (A) and real-time PCR analysis of ferroptosis-related markers (B) on LCN2-knockdown cells (HT29-sh1, 2). Level of intracellular and total ROS (C, D), mitochondrial membrane potential (MMP) (E), and ferrous iron ($Fe^{2+}$) (F) detection in LCN2-knockdown cells (HT29). (G) Quantification of the fold change of dual luciferase promoter reporter assays of FPN in corresponding cells. Target mRNA levels were normalized to GAPDH. Mean ± SD from at least three independent experiments. *P < .05, **P < .01, ***P < .001, ns, not significant.

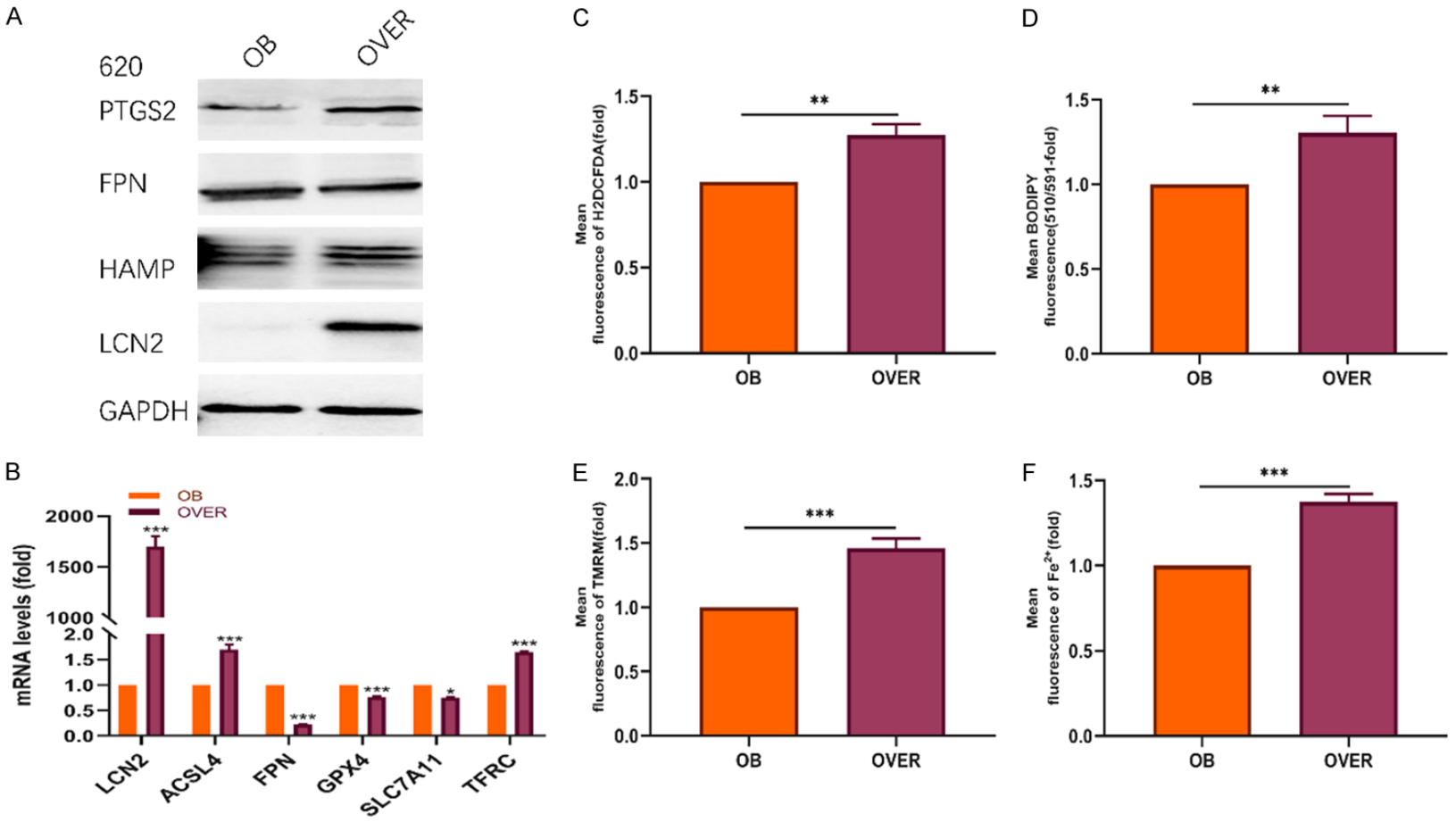


**Figure 2.** LCN2 upregulates ferroptosis markers in colorectal cancer (CRC) cells. PTGS2, FPN, HAMP and LCN2 expression measured by western blots (A) and mRNA levels analysis of key factors of ferroptosis (B) in LCN2-overexpressing cells of SW620 (OVER, vector control-OB). (C-F) Intracellular and total ROS levels, MMP, and $Fe^{2+}$ analysis in corresponding cells. Mean ± SD, *P < .05, **P < .01, ***P < .001.

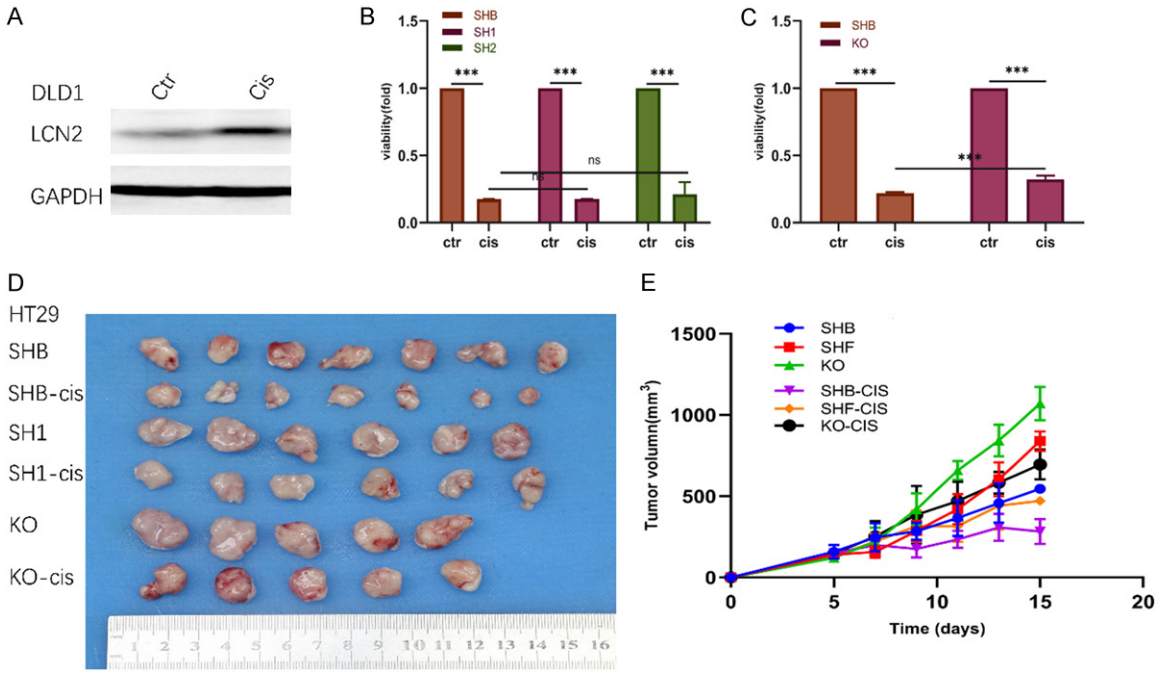


**Figure 3.** Genetic decrease of LCN2 disrupts the survival ability of CRC cells and anti-tumor effect of cisplatin. (A) Changes of LCN2 expression in CRC cells of DLD1 treated with cisplatin (30 μM, 48 h). (B, C) Proliferation detection in shLCN2-1, 2 and LCN2-knockout (LCN2-KO) cells after cisplatin treatment (30 μM) for 48 h. Representative images (D) and volume measurements (E) of corresponding HT29 tumors in BALB/c nude mice treated as indicated. Mean ± SD, *P < .05, **P < .01, ***P < .001, ns, not significant.

were observed in CRC tumors compared to normal tissues (**Figure 5I**, **5J**). Notably, among cases which colonoscopy biopsy tissues were reserved before chemotherapy, immunohistochemical detection showed that the expression rate of LCN2 in TRG1 cases (94.12%) was significantly higher than that in TRG3 cases (60%) (Figure S5A), while FPN expression rate was markedly lower in TRG1 cases (47.06% vs. 90%) (**Table 1**). Further analysis revealed a significant negative correlation between LCN2 and FPN, although without significant statistical significance (**Table 2**). Likewise, immunohistochemical measurement of tumor xenografts showed enhanced staining of FPN in shLCN2-1 and LCN2-KO tumors and tumors with cisplatin treatment (Figure S4), which is in accordance with our results observed in cells. These results suggested that loss of LCN2 may act as a negative regulator in cisplatin-stimulated ferroptosis via manipulating FPN expression.

*Loss of LCN2 renders insensitivity of CRC cells to cisplatin via promoting FPN expression through activating NF-κB*

Our previous results showed enhanced phospho-NF-κB p65 (p-p65) expression and capacity of cell proliferation, migration and invasion in shLCN2 CRC cells [16]. To further investigate mechanisms underlying LCN2/FPN pathway modulated ferroptosis in the presence of cisplatin. The cells were then confirmed by evaluating NF-κBp65 (p65) activity, which plays a pivotal role in almost all cancers. However, its role in ferroptosis remains to be elucidated yet. To our surprise, p-p65 expression was also be augmented by cisplatin (**Figures 6A**, S3F). Knockdown of p65 by siRNA reversed the expression of PTGS2 and FPN (**Figure 6B**, **6C**), and the changes of ferroptosis-related genes (Figures S5B and S6), lipid ROS, $Fe^{2+}$ level and MMP after cisplatin treatment in shLCN2 cells (**Figure 6D-F**). The luciferase reporter assay also confirmed that interfering with p65 could significantly ameliorate the increasing activity of FPN promoter by cisplatin (**Figure 6G**), implying that shLCN2 may inhibit ferroptosis through triggering FPN expression induced by p65 activation, attenuating the subsequent Fenton reaction, therefore, enhancing the insensitivity of CRC cells to cisplatin.

Collectively, our results indicate that loss of LCN2 expression exhibits as a suppressor of ferroptosis by activating the p65/FPN signaling

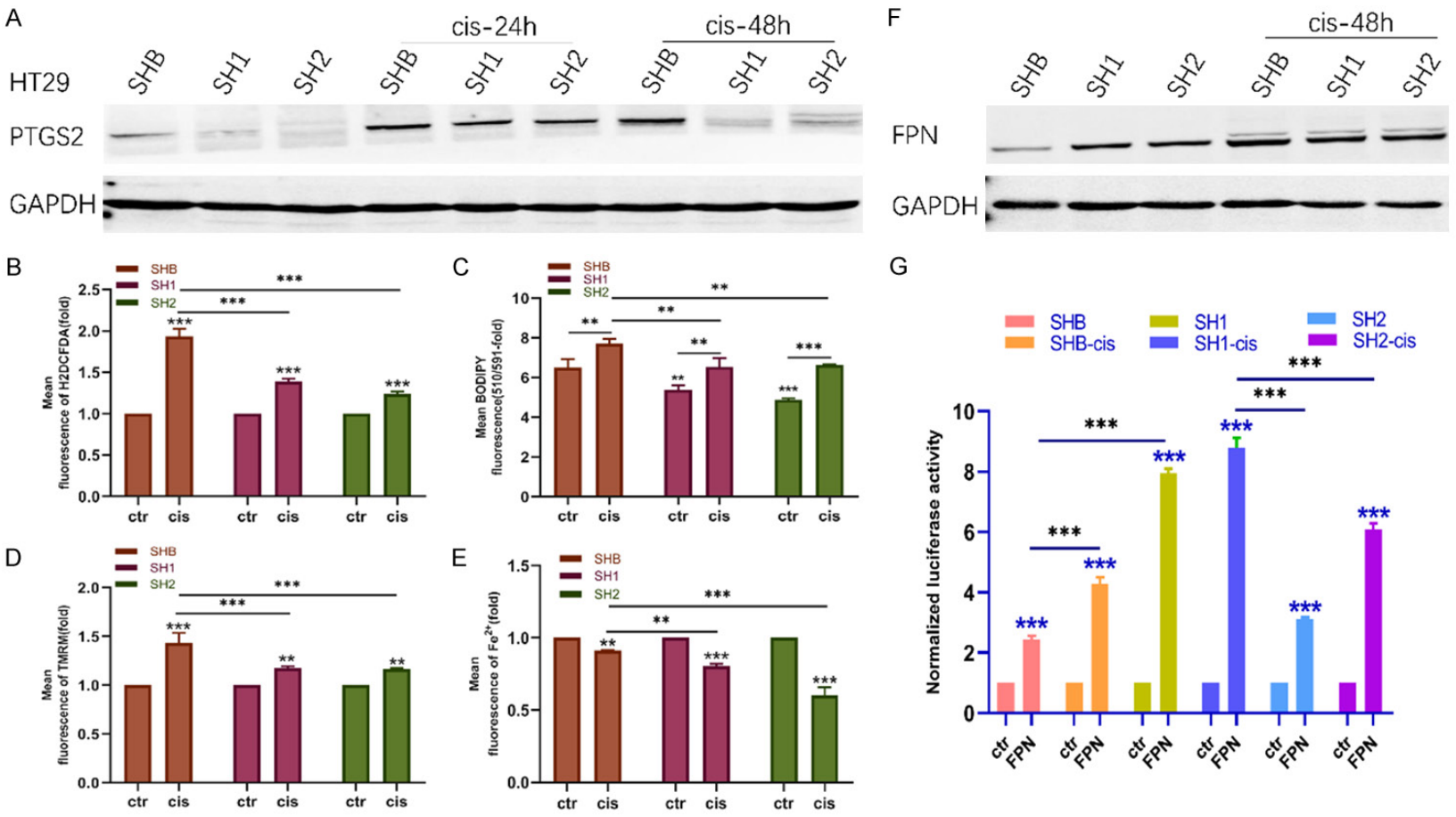


**Figure 4.** Knockdown of LCN2 mediates resistance of cisplatin-induced ferroptosis. A, F. Changes of PTGS2 and FPN expression in shLCN2 cells treated with cisplatin for indicated time (30 μM). B-E. Intracellular and total ROS level, MMP, and $Fe^{2+}$ detection in corresponding cells (cisplatin, 30 μM for 24 h). G. Quantification of the fold change of dual luciferase promoter reporter assays of FPN in shLCN2-1 cells with cisplatin (30 μM, 24 h). Mean ± SD, **P < .01, ***P < .001.

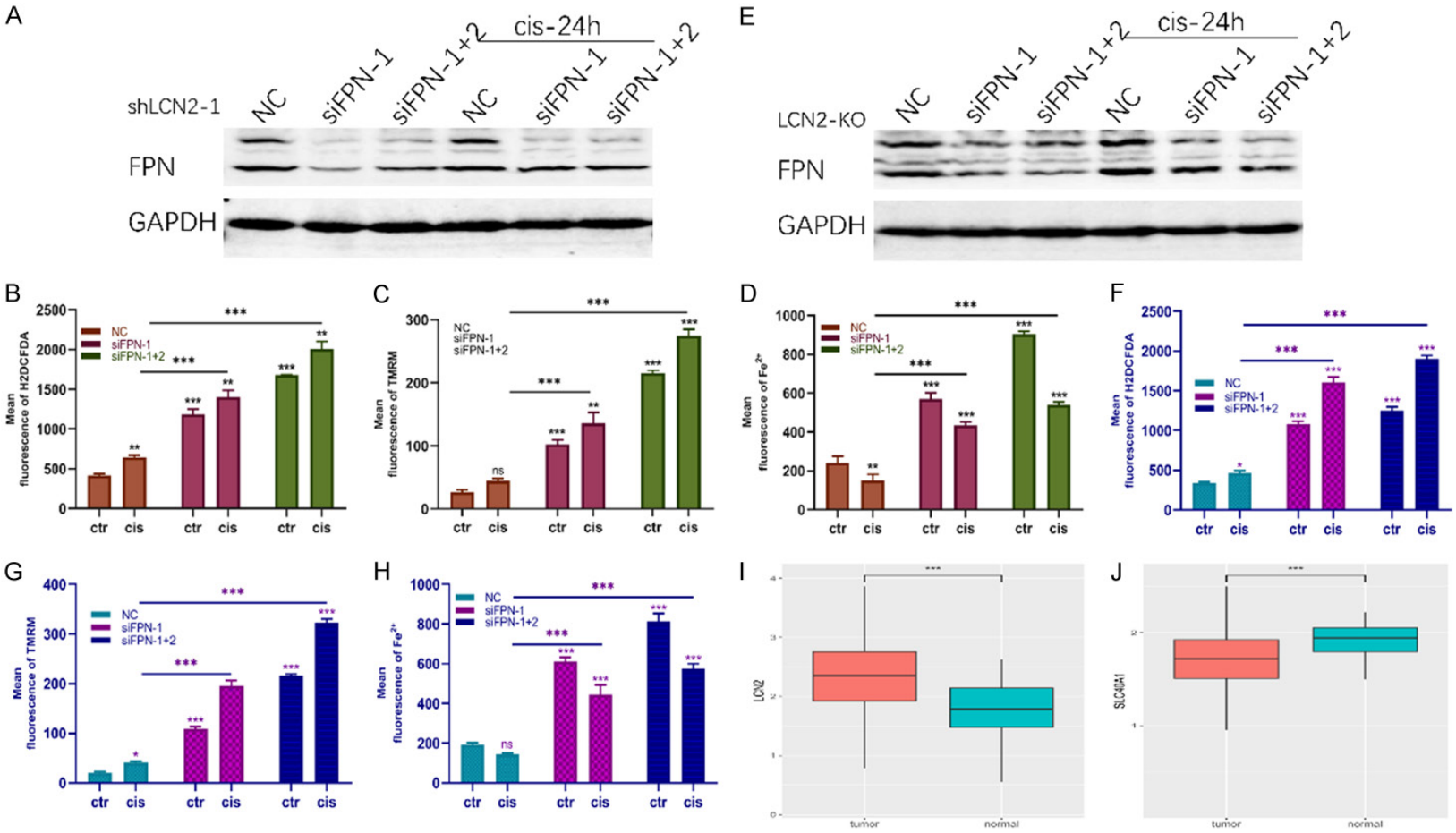


**Figure 5.** Decrease the expression of FPN reverses LCN2-knockdown induced inhibition of ferroptosis with cisplatin. (A, E) FPN expression measurement in shLCN2 or LCN2-KO cells after transfecting with specific siRNA, and treated with cisplatin (30 μM) for 24 h. Intracellular and total ROS levels, MMP, and $Fe^{2+}$ contents detection in shLCN2 (B-D) and LCN2-KO (F-H) cells with cisplatin treatment (30 μM, 24 h). (I, J) The expression of LCN2 and FPN (SLC40A1) in normal and CRC tissues in TCGA database. NC: negative control; ctr: control; Mean ± SD, *P < .05, **P < .01, ***P < .001, ns, not significant.

**Table 1.** Immunohistochemistry staining of Lipocalin2 (LCN2) and ferroportin (FPN) in clinical biopsy tissues before receiving chemotherapy treatment

| Variable | Score of chemotherapy effect (TRG system, n) | |
|---|---|---|
| | TRG1 (n = 17) | TRG3 (n = 20) |
| LCN2 | 94.12% | 60% |
| FPN | 47.06% | 90% |

Chemotherapy effect was evaluated by tumor regression grade (TRG) score system in radical surgery tissues after chemotherapy by two independent pathologists.

pathway mediated Fenton reaction, mitigating the sensitivity of CRC cells to cisplatin-induced ferroptosis (**Figure 7**). Notably, LCN2 and FPN expression may be a promising biomarker for chemotherapy effect of CRC patients. Our findings may provide new and unique insights for chemotherapeutic effect for CRC patients.

## Discussion

Here, we provide new evidence directly showing that loss of LCN2 expression prevents CRC cells from undergoing ferroptosis by targeting the NF-κB/FPN signaling pathway, which modulates intracellular $Fe^{2+}$ accumulation induced Fenton reaction, more importantly, enhancing cisplatin vulnerability in CRC. These findings identify the LCN2/NF-κB/FPN signaling pathway as highly suitable candidates for chemotherapeutic agents for CRC patients.

Our previous study showed that LCN2 was highly expressed in CRC tissues. More importantly, Higher expression of LCN2 together with negative NF-κB expression was positively related to favorable prognosis [16].

As one of the most widely used chemotherapy drugs, recent researches indicated that the modulation role of cisplatin in ferroptosis. Moreover, LCN2 was identified as a core factor in iron metabolism due to its capacity of iron-sequestering. Nevertheless, understanding of the role of LCN2 in cisplatin-mediated ferroptosis has been complicated by the contradictory findings in different researches. On the one hand, reduced LCN2 expression could counteract cisplatin effects in oral squamous cell carcinoma [19] and ameliorate erastin-mediated ferroptosis, meanwhile, increase cisplatin vulnerability in breast cancer cells [20].

**Table 2.** Correlation analysis between the expression of immunohistochemical staining of LCN2 and FPN in clinical CRC tissues before receiving chemotherapy treatment

| | Variable | |
|---|---|---|
| LCN2 | FPN (TRG1, n = 17) | FPN (TRG3, n = 20) |
| r value | -0.333 | -0.272 |
| *p* value | 0.197 | 0.233 |

Additionally, in prostate cancer, LCN2-KO enhances cisplatin-induced apoptosis while reducing cancer cell migration ability [21]. On the other hand, LCN2 has been reported as a biomarker for cisplatin-induced acute kidney injury or nephrotoxicity [22-24], and elevated LCN2 level could protect the kidney cells against cisplatin-induced injury [25]. Besides, knockdown of LCN2 significantly promotes the ability of survival, proliferation, migration and chemoresistance in oral cancer cell [26]. The mechanisms of LCN2 underlying cisplatin-induced ferroptosis needs further exploration.

Our results revealed that LCN2 expression was significantly upregulated by cisplatin both in vitro and in vivo, loss of LCN2 mitigated the level of lipid ROS, MMP, $Fe^{2+}$ content and PTGS2 expression in CRC cells, subsequently prevented cisplatin-stimulated ferroptosis process.

Although the involvement of the NF-κB signaling pathway in ferroptosis and chemotherapy has been reported, the mechanisms involved were not clear yet. Furthermore, the regulation of LCN2 in the NF-κB signaling pathway on cisplatin-induced ferroptosis in cancer had not been reported. NF-κB was indicated to be a prominent factor that takes part in almost all cancers [27, 28]. Research showed that phosphorylation of NF-κB inhibits ferroptosis in ulcerative colitis [29], which increases the risk of CRC by causing a cellular immune response and accumulating genetic alterations that might trigger specific oncogenic pathways [30-32]. Moreover, activated NF-κB activity attenuates ferroptosis [18] and enhance chemoresistance of cancer cells to cisplatin in multiple cancers [19, 33, 34]. Our results demonstrated that decreased LCN2 expression significantly increases the expression of phosphorylation p65, which is consistent with our previous results in CRC cells. In addition, knockdown of p65 by siRNA could partially rescue the inhibi-

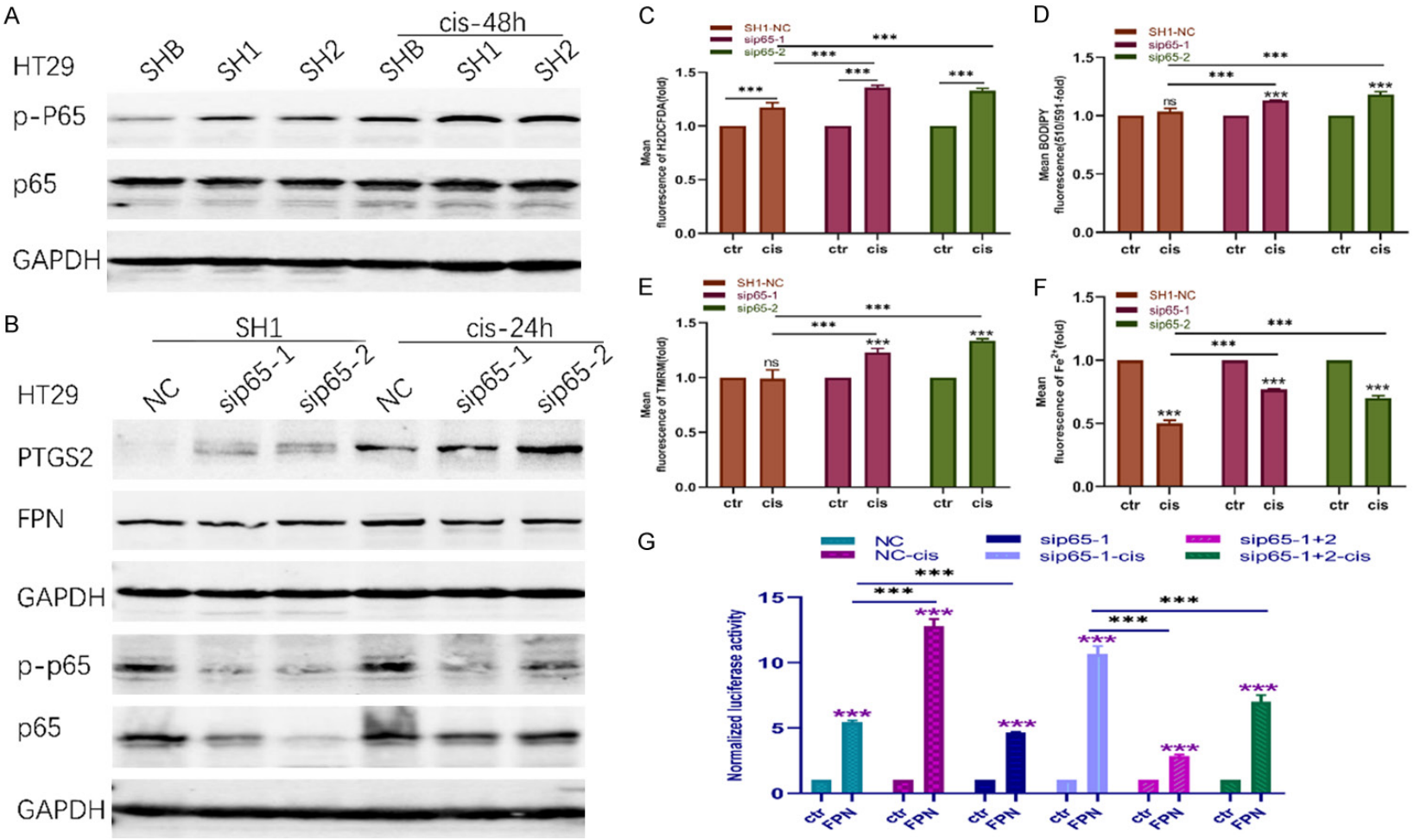


**Figure 6.** Reduced expression of LCN2 attenuates cisplatin-induced ferroptosis through activating NF-κB/FPN signaling pathway. (A) Phospho-p65 (p-p65) expression of corresponding cells with cisplatin for indicated time (30 μM). (B) Changes of PTGS2, FPN, p-p65 and p65 expression after knockdown by specific siRNA of p65 (sip65) in corresponding cells, and underlying cisplatin treatment (30 μM, 24 h). For measuring ferroptosis levels, shLCN2 cells with knockdown of p65 by siRNA were treated with cisplatin (30 μM), after 24 h, the levels of lipid peroxidation (C, D), MMP (E) and $Fe^{2+}$ (F) were determined. (G) Fold change of quantification of dual luciferase promoter reporter assay of FPN in corresponding cells treated with cisplatin (30 μM, 24 h). NC: negative control; Mean ± SD, ***P < .001, ns, no significance.

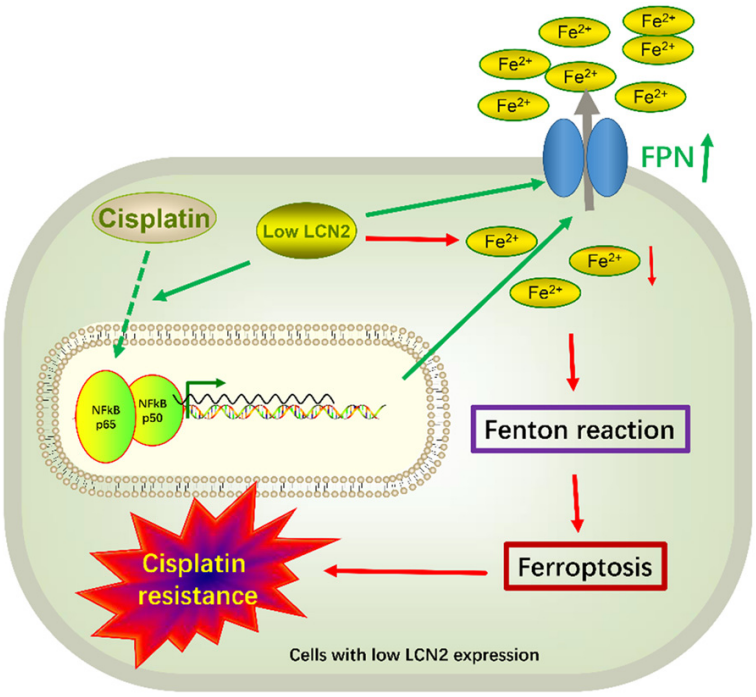


**Figure 7.** Working model of low expression of LCN2-induced insensitivity of CRC cells to cisplatin treatment. Low expression of LCN2 activates NF-κBp65, leading to the upregulation of FPN expression, and consequent suppression of Fenton reaction induced by $Fe^{2+}$ reduction underlying cisplatin treatment, which subsequently attenuates cisplatin-induced ferroptosis and eventually leading to cisplatin resistance to CRC cells. Meanwhile, cisplatin could also promote NF-κBp65/FPN signaling pathway and decrease $Fe^{2+}$ accumulation, this effect may contribute to chemoresistance of CRC cells.

tion of ferroptosis caused by reduced expression of LCN2 under the treatment of cisplatin, suggesting that loss of LCN2 prevented cisplatin-induced ferroptosis and enhanced chemoresistance of CRC cells against cisplatin, partially through activating NF-κB pathway.

As the reduced $Fe^{2+}$ accumulation and elevated FPN expression were obtained after decreasing LCN2 expression in our study, we next test the possibility that LCN2-NF-κB signaling pathway participates in the modulation of FPN expression in ferroptosis in the treatment of cisplatin. As shown in our results, inhibition of NF-κB reverted the increased expression of FPN after treatment with cisplatin, as well as the enhanced promoter activity of FPN in shLCN2 or LCN2-KO cells. These results indicated that reduced expression of LCN2 may suppress cisplatin-induced ferroptosis and increase cisplatin vulnerability, via activating NF-κB-FPN pathway, subsequently inhibiting $Fe^{2+}$ accumulation-regulated Fenton reaction.

Interestingly, we observed that cisplatin could also decrease the accumulation of intracellular $Fe^{2+}$, and promote NF-κB pathway. To our surprise, it did not significantly affect the progress of cisplatin-induced ferroptosis. This may be related to the previously report that cisplatin primarily regulates ferroptosis through activating the GSH-GPX4 pathway [35]. Whereas, one study has observed the increased levels of $Fe^{2+}$ in renal injury in mice [36]. Therefore, the regulation role of cisplatin in iron metabolism needs more investigation.

More importantly, we identified two aspects of the clinical importance of LCN2 in CRC. First, patients with better chemotherapy effect (TRG1) showed higher LCN2 expression than that of TRG3. Second, immunohistochemical analysis of CRC tissues also showed that LCN2 expression was negatively correlated with FPN expression, due to the limited cases, we did not observe significant statistics significance, the investigation of the relationship between LCN2 and FPN still needs more effort. In our study, LCN2 inhibited ferroptosis of CRC cells in vitro, as well as tumor growth in vivo.

Collectively, these results clearly demonstrate that loss of LCN2 suppresses cisplatin-induced ferroptosis by provoking NF-κB/FPN pathway in CRC, which attenuates $Fe^{2+}$ induced Fenton reaction and enhances chemoresistance of CRC to cisplatin. Our study provides a new therapeutic sight in CRC patients with chemotherapy. Notably, LCN2 and FPN expression may be a promising biomarker of chemotherapy effect and chemoresistance in CRC.

## Acknowledgements

We are grateful to Professor Maode Lai for suggestions of the study, and providing cell lines of

colorectal cancer, and Professor Wei Ding and Professor Jing Zhang for helpful support of the experiments. This research was supported by National Natural Science Foundation of China under Grant No. 82002488, Zhejiang Provincial Natural Science Foundation of China under Grant Nos. LQ21H160020 and LQ19H160038, and Medical and Health Science and Technology Program of Zhejiang Province under Grant No. 2022RC145.

## Disclosure of conflict of interest

None.

## Abbreviations

CRC, Colorectal cancer; LCN2, Lipocalin2; Cis, cisplatin; NF-κB, Nuclear factor-kappa B; p65, Nuclear factor kappa-B p65; p-p65, Phosphorylated p65; FPN, ferroportin; TMRM, Tetramethylrhodamine, mitochondrial membrane potential (MMP) indicator; Ctr, blank control; SHB/OB, Blank control of shRNA/overexpression vector of LCN2; shLCN2, shRNA vector of LCN2; LCN2-KO, knockout vector of LCN2; TRG, tumor regression grade; TRG1, single cells or small groups of tumor cells were left; TRG3, extensive residual tumor with minimal or no regression were observed.

**Address correspondence to:** Dr. Meibao Feng, Department of Pathology, The First Affiliated Hospital, School of Medicine, Zhejiang University, #79 Qingchun Road, Hangzhou 310003, Zhejiang, P. R. China. Fax: +86-0571-87236362; E-mail: 11318069@zju.edu.cn

## References

[1] Siegel RL, Miller KD, Wagle NS and Jemal A. Cancer statistics, 2023. CA Cancer J Clin 2023; 73: 17-48.

[2] Wang D and Lippard SJ. Cellular processing of platinum anticancer drugs. Nat Rev Drug Discov 2005; 4: 307-320.

[3] Amable L. Cisplatin resistance and opportunities for precision medicine. Pharmacol Res 2016; 106: 27-36.

[4] Guo J, Xu B, Han Q, Zhou H, Xia Y, Gong C, Dai X, Li Z and Wu G. Ferroptosis: a novel anti-tumor action for cisplatin. Cancer Res Treat 2018; 50: 445-460.

[5] Dixon SJ, Lemberg KM, Lamprecht MR, Skouta R, Zaitsev EM, Gleason CE, Patel DN, Bauer AJ, Cantley AM, Yang WS, Morrison B 3rd and Stockwell BR. Ferroptosis: an iron-dependent form of nonapoptotic cell death. Cell 2012; 149: 1060-1072.

[6] Stockwell BR, Friedmann Angeli JP, Bayir H, Bush AI, Conrad M, Dixon SJ, Fulda S, Gascon S, Hatzios SK, Kagan VE, Noel K, Jiang X, Linkermann A, Murphy ME, Overholtzer M, Oyagi A, Pagnussat GC, Park J, Ran Q, Rosenfeld CS, Salnikow K, Tang D, Torti FM, Torti SV, Toyokuni S, Woerpel KA and Zhang DD. Ferroptosis: a regulated cell death nexus linking metabolism, redox biology, and disease. Cell 2017; 171: 273-285.

[7] Stockwell BR, Jiang X and Gu W. Emerging mechanisms and disease relevance of ferroptosis. Trends Cell Biol 2020; 30: 478-490.

[8] Jiang X, Stockwell BR and Conrad M. Ferroptosis: mechanisms, biology and role in disease. Nat Rev Mol Cell Biol 2021; 22: 266-282.

[9] Yang WS and Stockwell BR. Ferroptosis: death by lipid peroxidation. Trends Cell Biol 2016; 26: 165-176.

[10] Gao J, Luo T and Wang J. Gene interfered-ferroptosis therapy for cancers. Nat Commun 2021; 12: 5311.

[11] Wang D, Li X, Jiao D, Cai Y, Qian L, Shen Y, Lu Y, Zhou Y, Fu B, Sun R, Tian Z, Zheng X and Wei H. LCN2 secreted by tissue-infiltrating neutrophils induces the ferroptosis and wasting of adipose and muscle tissues in lung cancer cachexia. J Hematol Oncol 2023; 16: 30.

[12] Gupta U, Ghosh S, Wallace CT, Shang P, Xin Y, Nair AP, Yazdankhah M, Strizhakova A, Ross MA, Liu H, Hose S, Stepicheva NA, Chowdhury O, Nemani M, Maddipatla V, Grebe R, Das M, Lathrop KL, Sahel JA, Zigler JS Jr, Qian J, Ghosh A, Sergeev Y, Handa JT, St Croix CM and Sinha D. Increased LCN2 (lipocalin 2) in the RPE decreases autophagy and activates inflammasome-ferroptosis processes in a mouse model of dry AMD. Autophagy 2023; 19: 92-111.

[13] Deng L, He S, Li Y, Ding R, Li X, Guo N and Luo L. Identification of Lipocalin 2 as a potential ferroptosis-related gene in ulcerative colitis. Inflamm Bowel Dis 2023; 29: 1446-1457.

[14] Luo L, Deng L, Chen Y, Ding R and Li X. Identification of Lipocalin 2 as a ferroptosis-related key gene associated with hypoxic-ischemic brain damage via STAT3/NF-κB signaling pathway. Antioxidants (Basel) 2023; 12: 186.

[15] Liu X, Li Y, Chen S, Yang J, Jing J, Li J, Wu X, Wang J, Wang J, Zhang G, Tang Z and Nie H. Dihydromyricetin attenuates intracerebral hemorrhage by reversing the effect of LCN2 via the system Xc- pathway. Phytomedicine 2023; 115: 154756.

[16] Feng M, Feng J, Chen W, Wang W, Wu X, Zhang J, Xu F and Lai M. Lipocalin2 suppresses metastasis of colorectal cancer by attenuating NF-κB-dependent activation of snail and epi-

thelial mesenchymal transition. Mol Cancer 2016; 15: 77.
[17] Li S, He Y, Chen K, Sun J, Zhang L, He Y, Yu H and Li Q. RSL3 drives ferroptosis through NF-kappaB pathway activation and GPX4 depletion in glioblastoma. Oxid Med Cell Longev 2021; 2021: 2915019.
[18] Yao F, Deng Y, Zhao Y, Mei Y, Zhang Y, Liu X, Martinez C, Su X, Rosato RR, Teng H, Hang Q, Yap S, Chen D, Wang Y, Chen MM, Zhang M, Liang H, Xie D, Chen X, Zhu H, Chang JC, You MJ, Sun Y, Gan B and Ma L. A targetable LIFR-NF-kappaB-LCN2 axis controls liver tumorigenesis and vulnerability to ferroptosis. Nat Commun 2021; 12: 7333.
[19] Huang Z, Zhang Y, Li H, Zhou Y, Zhang Q, Chen R, Jin T, Hu K, Li S, Wang Y, Chen W and Huang Z. Vitamin D promotes the cisplatin sensitivity of oral squamous cell carcinoma by inhibiting LCN2-modulated NF-kappaB pathway activation through RPS3. Cell Death Dis 2019; 10: 936.
[20] Valashedi MR, Roushandeh AM, Tomita K, Kuwahara Y, Pourmohammadi-Bejarpasi Z, Kozani PS, Sato T and Roudkenar MH. CRISPR/Cas9-mediated knockout of Lcn2 in human breast cancer cell line MDA-MB-231 ameliorates erastin-mediated ferroptosis and increases cisplatin vulnerability. Life Sci 2022; 304: 120704.
[21] Rahimi S, Roushandeh AM, Ebrahimi A, Samadani AA, Kuwahara Y and Roudkenar MH. CRISPR/Cas9-mediated knockout of Lcn2 effectively enhanced CDDP-induced apoptosis and reduced cell migration capacity of PC3 cells. Life Sci 2019; 231: 116586.
[22] Mishra J, Mori K, Ma Q, Kelly C, Barasch J and Devarajan P. Neutrophil gelatinase-associated lipocalin: a novel early urinary biomarker for cisplatin nephrotoxicity. Am J Nephrol 2004; 24: 307-315.
[23] Wang W, Li Z, Chen Y, Wu H, Zhang S and Chen X. Prediction value of serum NGAL in the diagnosis and prognosis of experimental acute and chronic kidney injuries. Biomolecules 2020; 10: 981.
[24] Jelinek MJ, Lee SM, Wyche Okpareke A, Wing C, Koyner JL, Murray PT, Stadler WM and O'Donnell PH. Predicting acute renal injury in cancer patients receiving cisplatin using urinary neutrophil gelatinase-associated lipocalin and cystatin C. Clin Transl Sci 2018; 11: 420-427.
[25] Halabian R, Roudkenar MH, Jahanian-Najafabadi A, Hosseini KM and Tehrani HA. Co-culture of bone marrow-derived mesenchymal stem cells overexpressing lipocalin 2 with HK-2 and HEK293 cells protects the kidney cells against cisplatin-induced injury. Cell Biol Int 2015; 39: 152-163.
[26] Monisha J, Roy NK, Padmavathi G, Banik K, Bordoloi D, Khwairakpam AD, Arfuso F, Chinnathambi A, Alahmadi TA, Alharbi SA, Sethi G, Kumar AP and Kunnumakkara AB. NGAL is downregulated in oral squamous cell carcinoma and leads to increased survival, proliferation, migration and chemoresistance. Cancers (Basel) 2018; 10: 228.
[27] Sen R and Baltimore D. Multiple nuclear factors interact with the immunoglobulin enhancer sequences. Cell 1986; 46: 705-716.
[28] Ben-Neriah Y and Karin M. Inflammation meets cancer, with NF-κB as the matchmaker. Nat Immunol 2011; 12: 715-723.
[29] Xu M, Tao J, Yang Y, Tan S, Liu H, Jiang J, Zheng F and Wu B. Ferroptosis involves in intestinal epithelial cell death in ulcerative colitis. Cell Death Dis 2020; 11: 86.
[30] Shah SC and Itzkowitz SH. Colorectal cancer in inflammatory bowel disease: mechanisms and management. Gastroenterology 2022; 162: 715-730, e713.
[31] Rogler G. Chronic ulcerative colitis and colorectal cancer. Cancer Lett 2014; 345: 235-241.
[32] Yashiro M. Ulcerative colitis-associated colorectal cancer. World J Gastroenterol 2014; 20: 16389-16397.
[33] Xie R, Cheng L, Huang M, Huang L, Chen Z, Zhang Q, Li H, Lu J, Wang H, Zhou Q, Huang J, Chen X and Lin T. NAT10 drives cisplatin chemoresistance by enhancing ac4C-associated DNA repair in bladder cancer. Cancer Res 2023; 83: 1666-1683.
[34] Wang S, Chen Z, Zhu S, Lu H, Peng D, Soutto M, Naz H, Peek R Jr, Xu H, Zaika A, Xu Z and El-Rifai W. PRDX2 protects against oxidative stress induced by H. pylori and promotes resistance to cisplatin in gastric cancer. Redox Biol 2020; 28: 101319.
[35] Min Y, Mao CQ, Chen S, Ma G, Wang J and Liu Y. Combating the drug resistance of cisplatin using a platinum prodrug based delivery system. Angew Chem Int Ed Engl 2012; 51: 6742-6747.
[36] Ikeda Y, Hamano H, Horinouchi Y, Miyamoto L, Hirayama T, Nagasawa H, Tamaki T and Tsuchiya K. Role of ferroptosis in cisplatin-induced acute nephrotoxicity in mice. J Trace Elem Med Biol 2021; 67: 126798.

**Table S1.** The sequences of the specific primers

| Gene | Sequences 5'-3' |
|---|---|
| LCN2-F | CTCCACCTCAGACCTGATCC |
| LCN2-R | ACATACCACTTCCCCTGGAAT |
| TFRC-F | GGCTACTTGGGCTATTGTAAAGG |
| TFRC-R | CAGTTTCTCCGACAACTTTCTCT |
| Ferroportin-F | CTACTTGGGGAGATCGGATGT |
| Ferroportin-R | CTGGGCCACTTTAAGTCTAGC |
| ACSL4-F | CATCCCTGGAGCAGATACTCT |
| ACSL4-R | TCACTTAGGATTTCCCTGGTCC |
| NF-κBp65-F | GGGCATGCGCTTCCGCTACA |
| NF-κBp65-R | TCCCCACGCTGCTCTTCTTGGA |
| PTGS2-F | CCGCAGTTGATACTGACGCTC |
| PTGS2-R | GCGCAGTTTACGCTGTCTAGC |
| FTH-F | ACTGATGAAGCTGCAGAACC |
| FTH-R | GTCACCCAATTCTTTGATGG |
| SLC7A11-F | CCTTTCAAGGTGCCACTGTT |
| SLC7A11-F | TCCCTATTTTGTGTCTCCCCTT |
| GPX4-F | TAGAAATAGTGGGGCAGGTCC |
| GPX4-R | CGTCAAATTCGATATGTTCAGC |
| GAPDH-F | TGCACCACCAACTGCTTAGC |
| GAPDH-R | GGCATGGACTGTGGTCATGAG |

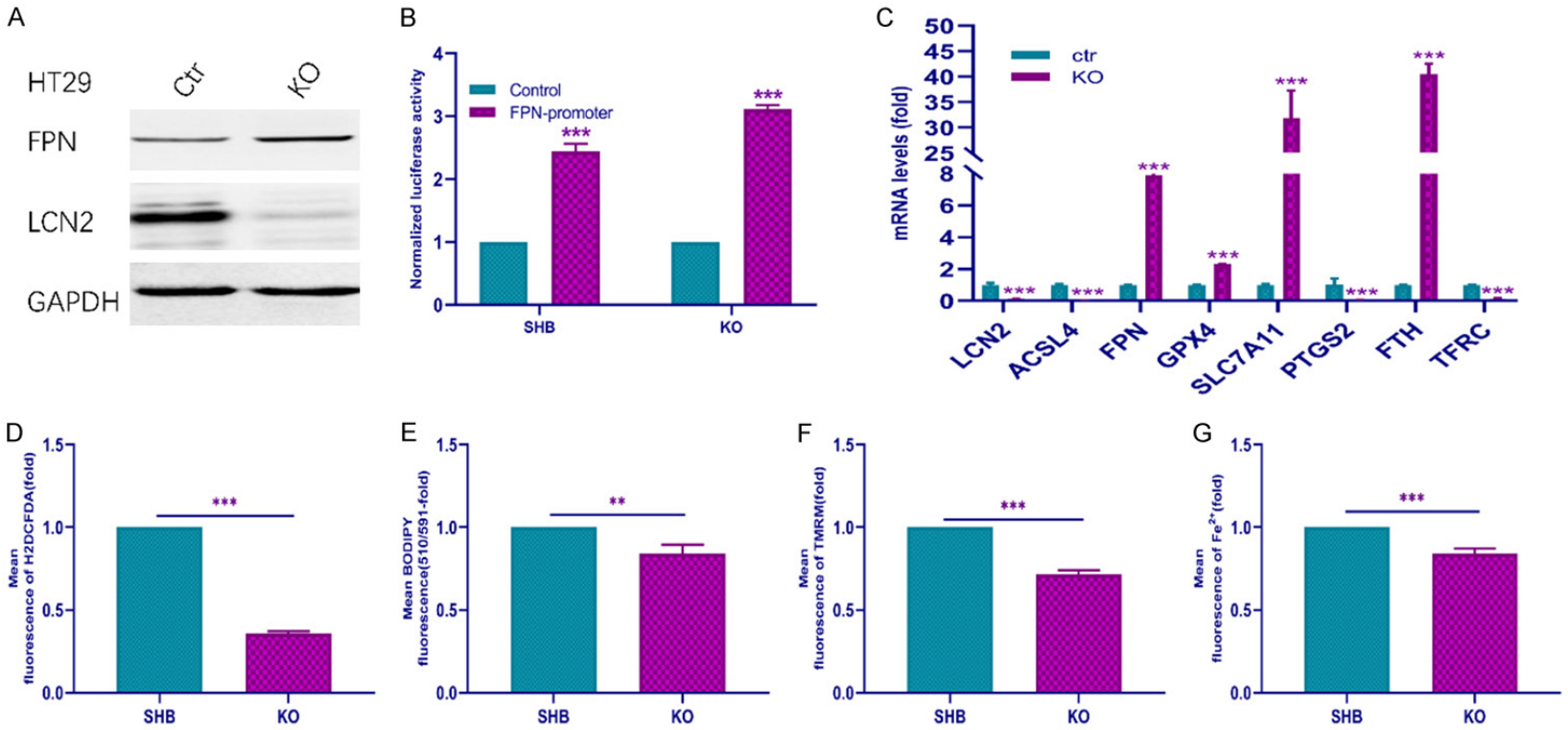


**Figure S1.** FPN expression and promoter activity of LCN2-KO and control cells (ctr, A, B). (C) Ferroptosis markers changes of mRNA levels (C), lipid ROS (D, E), MMP detection (F) and $Fe^{2+}$ levels (G) in corresponding cells. Target mRNA levels were normalized to GAPDH. Mean ± SD, **P < .01, ***P < .001.

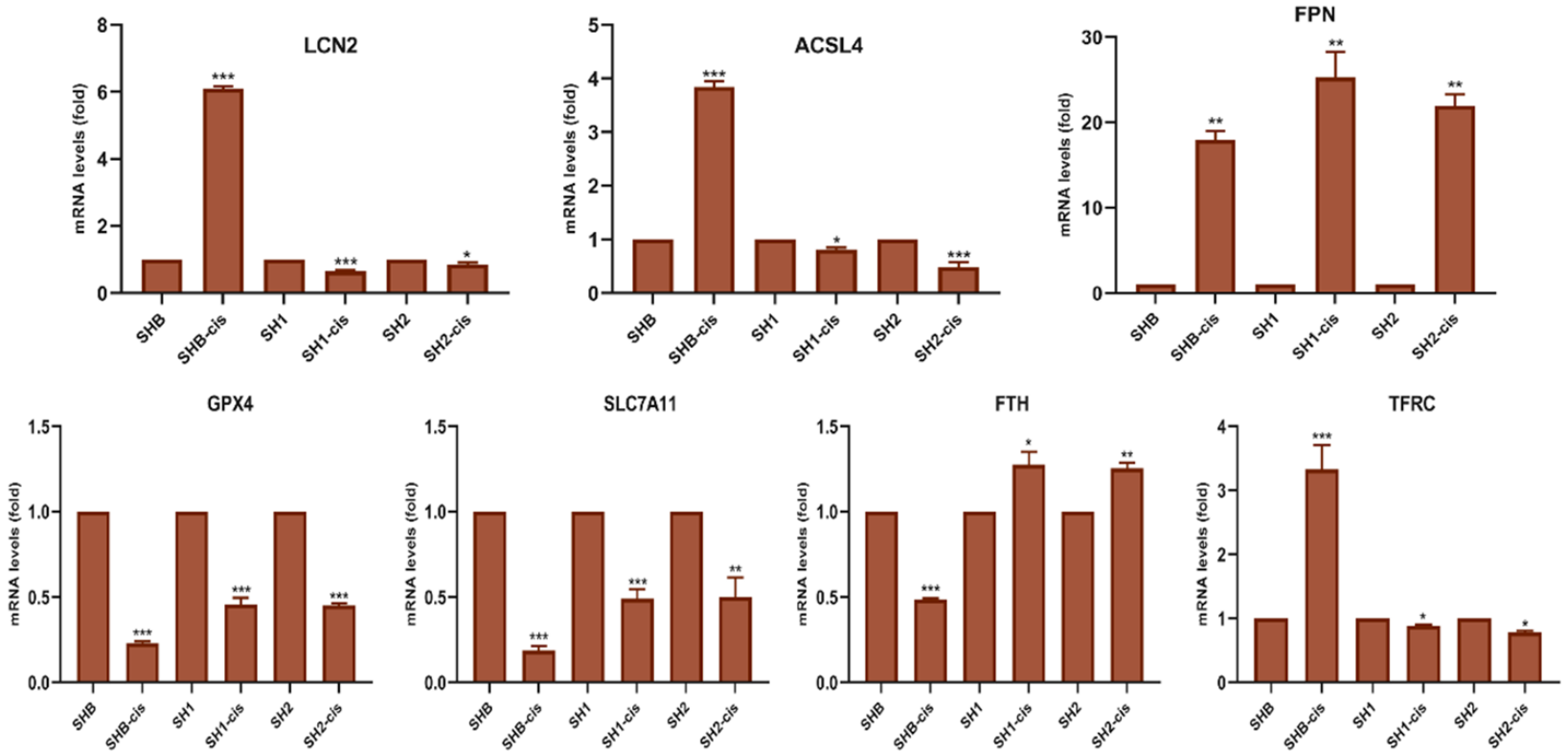


**Figure S2.** Real-time PCR analysis of mRNA levels of ferroptosis markers on LCN2-knockdown cells (sh1, 2) treated with cisplatin (30 μM) for 24 h. Mean ± SD, *P < .05, **P < .01, ***P < .001.

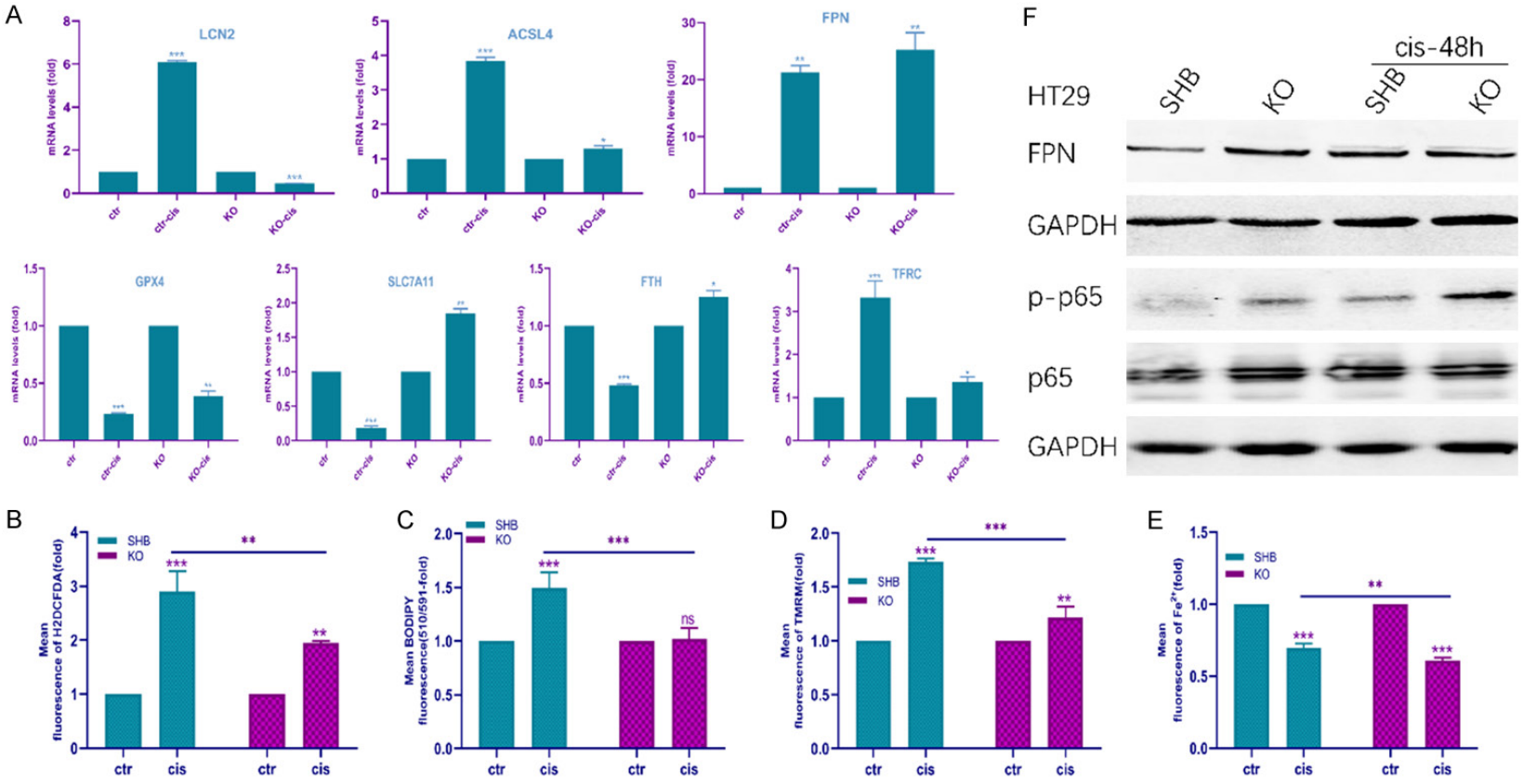


**Figure S3.** Knockout of LCN2 reduces ferroptosis induced by cisplatin. (A) Quantification of the fold change of mRNA levels of ferroptosis markers in corresponding cells with cisplatin (30 μM, 24 h). Lipid ROS levels (B, C), MMP detection (D) and $Fe^{2+}$ contents (E) in CRC cells treated with cisplatin (30 μM, 24 h). (F) Western blot analysis of FPN, p65 and p-p65 expression in LCN2-KO cells treated with cisplatin (30 μM) for indicated time. Ctr: control; Mean ± SD, *P < .05, **P < .01, ***P < .001, ns, no significance.

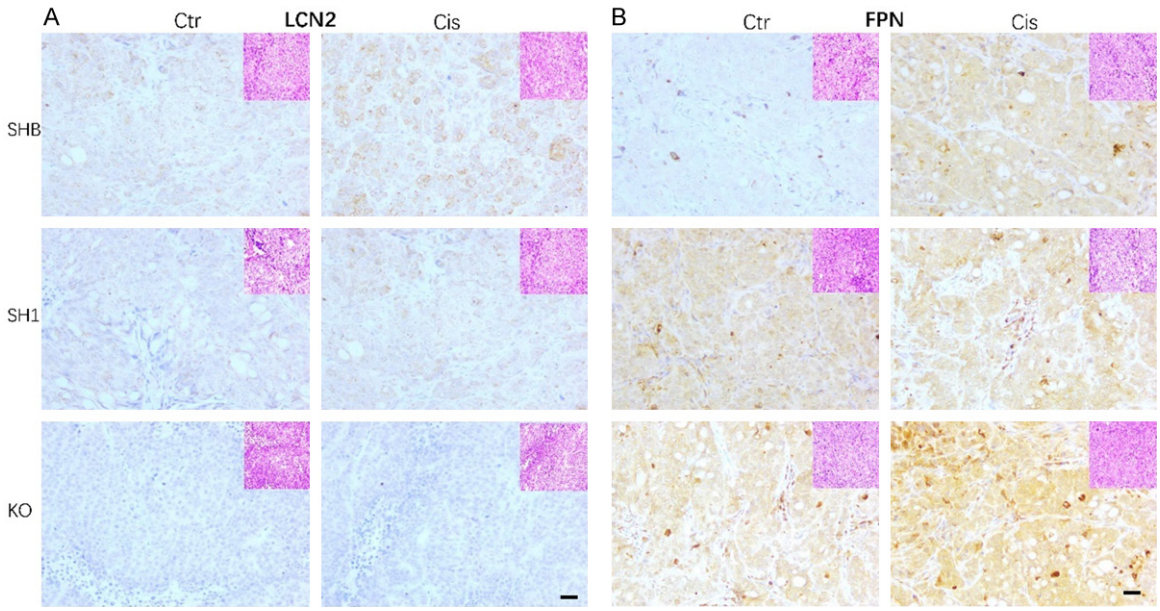


**Figure S4.** Immunohistochemical staining of LCN2 and FPN in mouse xenografts tissues. Expression of LCN2 (cytoplasm, A) and FPN (membrane and cytoplasm, B) of mouse xenografts tissues formed with HT29-SHB, shLCN2-1 and LCN2-KO cells and intraperitoneally injected with cisplatin (15 mg/kg) or the same amount of saline water for control every other day for the next 12 days. Hematoxylin-eosin (H&E) staining on top right corner. Scale bar 50 μm.

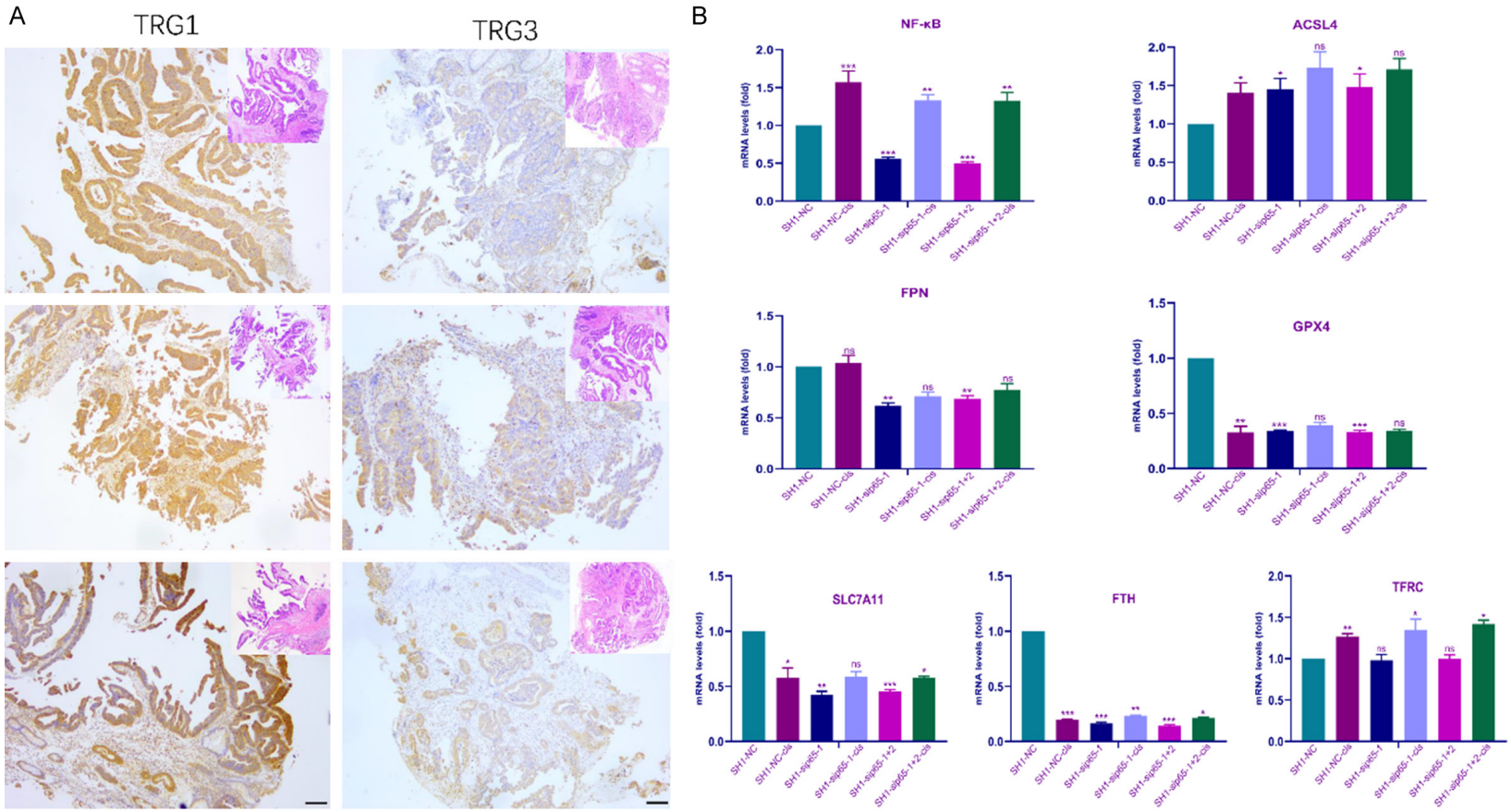


**Figure S5.** Immunohistochemical staining of LCN2 in clinical tissues of TRG1 and TRG3 (A). Changes of ferroptosis markers on mRNA levels of LCN2-knockdown (SH1) cells transfected with specific p65 siRNA (sip65), and treated with cisplatin (30 μM) for 24 h (B). Hematoxylin-eosin (H&E) staining on top right corner. Scale bar 1000 μm. Mean ± SD, *P < .05, **P < .01, ***P < .001, ns, no significance.

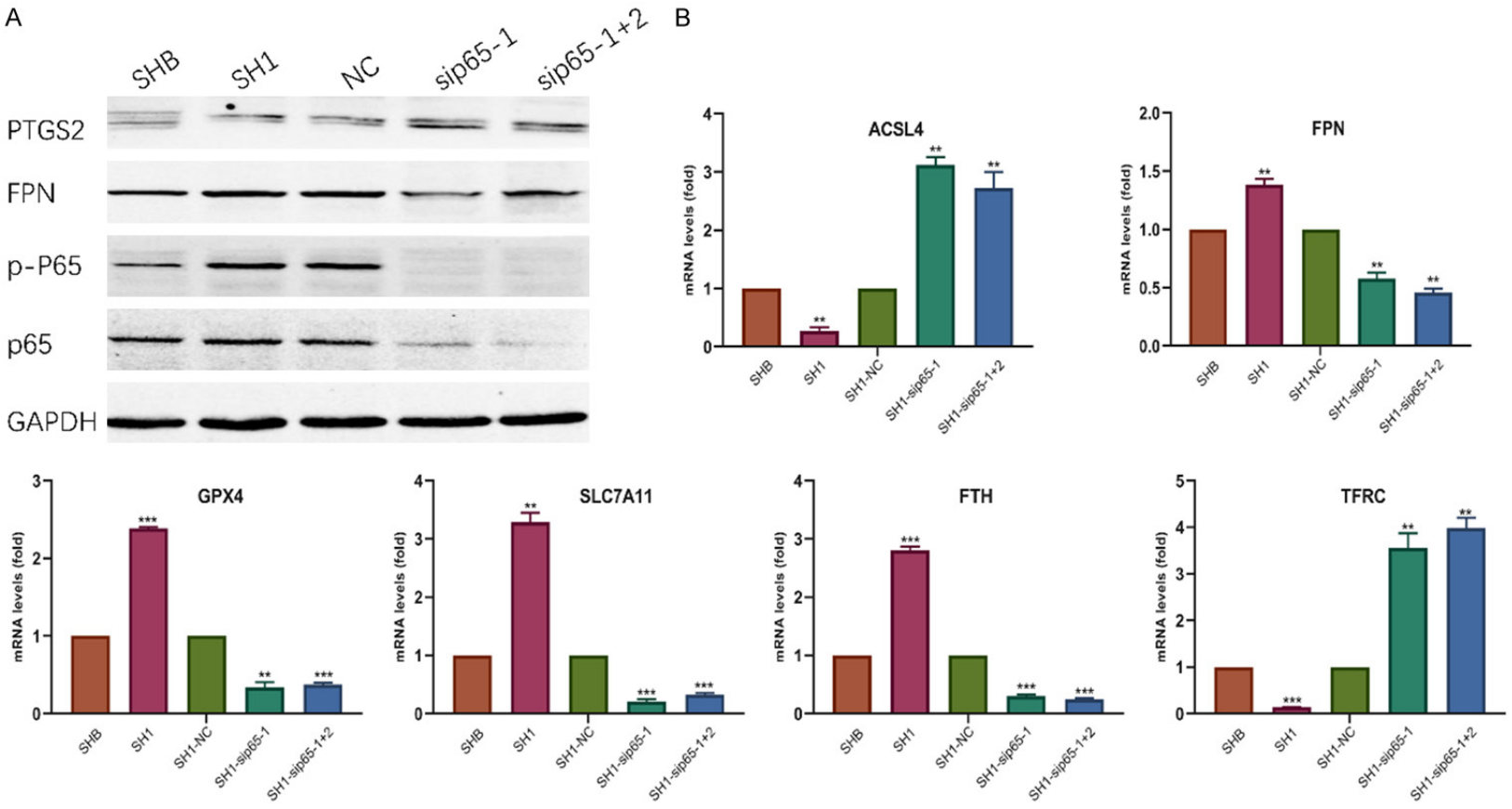


**Figure S6.** Changes of PTGS2, FPN, p-p65 and p65 expression (A), and mRNA levels of ferroptosis-related markers after knockdown by specific siRNA of p65 (sip65) in corresponding cells (B). Mean ± SD, **P < .01, ***P < .001.